nature materials

LETTERS

PUBLISHED ONLINE: 16 JANUARY 2011 | DOI: 10.1038/NMAT2929

Transient photoinduced 'hidden' phase in a manganite

Hirohiko Ichikawa[1], Shunsuke Nozawa[1,2], Tokushi Sato[1,2,3], Ayana Tomita[1,3], Kouhei Ichiyanagi[1†], Matthieu Chollet[3†], Laurent Guerin[1†], Nicky Dean[4], Andrea Cavalleri[4,5], Shin-ichi Adachi[1,2], Taka-hisa Arima[6], Hiroshi Sawa[2†], Yasushi Ogimoto[7], Masao Nakamura[7†], Ryo Tamaki[7], Kenjiro Miyano[7] and Shin-ya Koshihara[1,3*]

Photoinduced phase transitions are of special interest in condensed matter physics[1,2] because they can be used to change complex macroscopic material properties on the ultrafast timescale. Cooperative interactions between microscopic degrees of freedom greatly enhance the number and nature of accessible states, making it possible to switch electronic, magnetic or structural properties in new ways[2–9]. Photons with high energies, of the order of electron volts, in particular are able to access electronic states that may differ greatly from states produced with stimuli close to equilibrium[10]. In this study we report the photoinduced change in the lattice structure of a charge and orbitally ordered $Nd_{0.5}Sr_{0.5}MnO_3$ thin film using picosecond time-resolved X-ray diffraction. The photoinduced state is structurally ordered, homogeneous, metastable and has crystallographic parameters different from any thermodynamically accessible state. A femtosecond time-resolved spectroscopic study shows the formation of an electronic gap in this state. In addition, the threshold-like behaviour and high efficiency in photo-generation yield of this gapped state highlight the important role of cooperative interactions in the formation process. These combined observations point towards a 'hidden insulating phase' distinct from that found in the hitherto known phase diagram.

Theoretical studies of systems with competing degrees of freedom that are in a delicate equilibrium predict the formation of transient hidden phases that can be accessed by optical stimulation in the dynamical processes of photoinduced phase transitions[1,2,9,10] (PIPTs). Thus, strongly correlated materials are promising in searching for PIPTs because they are likely to have hidden phases that are energetically almost degenerate but thermally inaccessible. Many studies have investigated PIPTs and related phenomena, including hidden phases. Most of them used dynamic spectroscopic measurements to probe the local structural and electronic changes caused by transient states.

Nonlinear photoresponses in spectroscopic data provide strong support for the role of cooperative interactions in excited states, which is an expected characteristic of PIPTs (refs 1,2,9). Indeed, in the present study, the threshold-like behaviour in the photo-generation yield of the photoinduced state has also been confirmed by the optical method, as will be discussed later. However, to identify hidden phases induced by photoexcitation, it is essential to observe transient changes in the structural order that are distinct from known thermodynamic phases .

In the present study, $Nd_{0.5}Sr_{0.5}MnO_3$ (NSMO) is discussed as a typical example because its complex phase diagram exhibits important competition between charge, lattice, orbital and spin degrees of freedom[11–13]. An epitaxial thin film of NSMO on a (011) surface of perovskite $SrTiO_3$ (STO) (NSMO/STO(011)) was prepared by pulsed laser deposition[14,15]. The relation between the change in structure, including unit cell volume, induced by photoexcitation and the sensitive electronic response in this material was analysed by time-resolved X-ray diffraction (TR-XRD; Fig. 1a) and time-resolved optical spectroscopy[16]. The sample was 80 nm thick, which enabled us to excite and probe the same sample volume despite the exciting laser light and the X-rays having very different penetration depths (70 nm and 4 μm, respectively; Fig. 1a,b).

Thin films of NSMO/STO(011) exhibit a first-order orbital-ordered (OO) insulator–metal (IM) transition at $T_{IM} = 180$ K. X-ray diffraction analysis reveals that this transition is associated with uniform ordering of $d_{x^2-y^2}$ orbitals, which becomes a charge-ordered (CO) phase with a zigzag arrangement of $d_{3x^2-r^2}/d_{3y^2-r^2}$ orbitals (CO–OO) below $T_{CO-OO} = 160$ K (Fig. 1b); these are associated with A- and CE-type spin structures, respectively[17,18].

The e_g orbital shape is known to affect the out-of-plane elongation ratio (along the c axis) of the MnO_6 octahedra and in-plane distortion (within the a–b plane) of the MnO_4 plane around the Mn^{3+} site[19–22]. In the case of NSMO/STO(011), the a axis is locked to the STO substrate so that this lattice constant is fixed. In contrast, clear expansion along the b axis and contraction along the c axis below T_{IM} compared with the nearly isotropic M phase have been reported; they have been attributed to a noticeable reduction in the contribution of the $d_{3z^2-r^2}$ orbital[17,18]. A single Bragg diffraction peak of the M phase attributed to the (004)

[1]JST, ERATO, Tsukuba 305-0801, Japan, [2]Photon Factory, Institute of Materials Structure Science, High Energy Accelerator Research Organization, Tsukuba 305-0801, Japan, [3]JST, CREST & Department of Materials Science, Tokyo Institute of Technology, Meguro-ku, Tokyo 152-8551, Japan, [4]Department of Physics, University of Oxford, Clarendon Laboratory, Parks Road, Oxford, OX1 3PU, UK, [5]Max Planck Research Group for Structural Dynamics, University of Hamburg, Center For Free Electron Laser Science, c/o Desy - Bldg.49, Notkestrasse 85, 22607 Hamburg, Germany, [6]Institute of Multidisciplinary Research for Advanced Materials, Tohoku University, Sendai 980-8577, Japan, [7]JST, CREST & Research Center for Advanced Science and Technology, University of Tokyo, Tokyo 153-8904, Japan. †Present addresses: #609(7A2) Kiban Bldg., 5-1-5 Kashiwanoha, Kashiwa City, 277-8561, Chiba, Japan (K.I.); X-ray Science Division, Argonne National Lab., Argonne, Illinois 60439, USA (M.C.); European Synchrotron Radiation Facility (ESRF), 6 rue Jules Horowitz, BP220, 38043 Grenoble, France (L.G.); Department of Applied Physics, Nagoya University, Nagoya 464-8603, Japan (H.S.); Cross-Correlated Materials Research Group (CMRG), ASI, RIKEN, Wako, Saitama 351-0198, Japan (M.N.). *e-mail: skoshi@cms.titech.ac.jp.

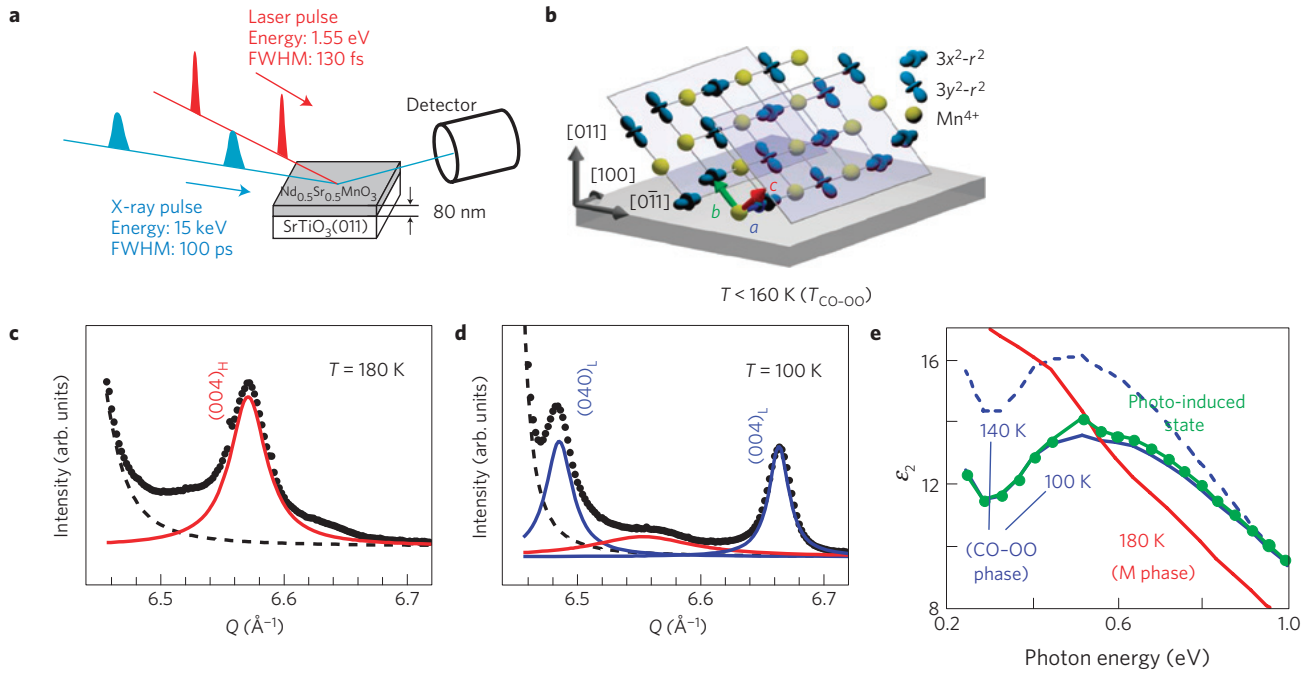

Figure 1 | X-ray diffraction patterns for M and CO–OO phases. a, Experimental set-up for 100-ps TR-XRD. Details of the system are presented in the Supplementary Information. **b**, A schematic view of crystal and orbital structures in the low-temperature CO–OO state. *a*, *b* and *c* are crystal axes in pseudocubic notation. In the present study, pseudocubic notation is used to facilitate discussion of structural deformation following the previous studies[17,18]. **c**, Intensity profile (filled circles) near the (004) reflection of NSMO in the high-temperature phase (labelled $(004)_H$) observed at 180 K. **d**, The $(004)_H$ peak splits into two peaks in the low-temperature phase, as indicated by the peaks labelled $(040)_L$ and $(004)_L$ measured at 100 K. Q denotes the magnitude of the scattering vector. The solid lines in **c** and **d** are Lorentzian fits to the data after subtracting the contribution (broken grey line) from the (004) peak of the STO substrate. **e**, Absorption spectra in the high-temperature M phase (red line) observed at 180 K and in the low-temperature CO–OO phase (blue line) at 100 and 140 K. Green dots represent the ε_2 spectrum observed 150 ps after photoexcitation, obtained from the $\Delta\varepsilon_2$ spectrum shown in Fig. 3.

reflection (the $(004)_H$ peak in Fig. 1c) splits into two peaks ($(040)_L$ and $(004)_L$ peaks in Fig. 1d), reflecting the lifting of degeneracy between the *b* and *c* axes. Furthermore, the Jahn–Teller distortion in the *a*–*b* plane in the CO–OO state produces superlattice reflections at (1/4 9/4 0) with intensities that vary as the square of the order parameters of the CO–OO state. Therefore, the *b*- and *c*-axis lattice constants, the (004) and (040) diffraction peak profiles, and the superlattice spot intensity form a suitable set of indicators for observing photo- and thermodynamic effects on the lattice structure and estimating photoinduced changes in distortions of the MnO_6 octahedra.

Studies of PIPTs in perovskite manganites have mainly focused on the IM transition induced by optical excitation, where the melting of the CO state and the associated structural changes are similar to those of the thermally induced phase transition, as this represents the simplest scenario[23]. In NSMO/STO(011), the thermally induced transition from the CO–OO state (the I phase) to the M phase is accompanied by a large spectral change due to the disappearance of the electronic gap, as shown in Fig. 1e. The broad absorption band in this photon energy region observed with light linearly polarized in the [100] direction is assigned to the charge transfer excitation between Mn^{3+} and Mn^{4+} ions[13]. Anticipating that photoexcitation would induce structural and spectral changes common to the thermally induced IM transition, we carried out time-resolved X-ray and spectroscopic studies of NSMO/STO(011) using a standard femto- and picosecond pump–probe set-up at 100 K (see Supplementary Information).

Figure 2a shows the temporal profiles of the photoinduced changes in lattice constant for the *b* and *c* axes observed at 100 K by TR-XRD with a time resolution of 100 ps (see Supplementary Information). The lattice constants start to change immediately after photoexcitation, peaking 250–300 ps later and then decaying with a time constant of 3 ns (dashed curve in Fig. 2a). Reflecting the observed photoinduced structural change, the estimated unit cell volume also shows changes (ΔV), as indicated by black circles in Fig. 2a. The observed structural change indicates the appearance of a state that may be assigned as a hidden phase. For confirmation and identification of the appearance of a hidden phase, of course, it is essential to verify that the photoinduced state is a unique phase with a structural order that cannot be achieved thermodynamically.

To observe the detailed lattice motion, Fig. 2c,d shows difference diffraction patterns (DDPs), that is, diffraction patterns from which the patterns at 100 K have been subtracted. Figure 2c shows DDPs at four temperatures above 100 K and Fig. 2d shows DDPs after photoexcitation at four different pump fluences. The top curve in Fig. 2c is a hypothetical DDP obtained by converting 3% of the CO–OO state at 100 K into the M phase at 180 K.

The coexistence of a small amount of nanoscale clusters in the M phase with the CO–OO host state (Fig. 1c and d) even at 100 K is an important and characteristic thermodynamic behaviour of NSMO/STO(011) in the ground state. Indeed, such coexistence of competing phases and/or occurrence of nanoscale phase separation has been discussed as an important thermodynamic property of the manganites, relating to the origin of colossal magneto-resistance[24]. A fraction of the M phase clusters is sensitive to simple temperature change (Fig. 2c); a temperature rise of only 10–15 K greatly increases the diffuse scattering intensity near $Q = 6.58$ Å^{-1}. This diffuse peak can thus be used as a highly sensitive temperature probe.

The DDPs in Fig. 2d differ noticeably from those in Fig. 2c. The salient characteristics are the complete absence of the diffuse peak profile (indicated by the light red band), which signifies the growth and coexistence of metallic clusters, and also the lack of broadening

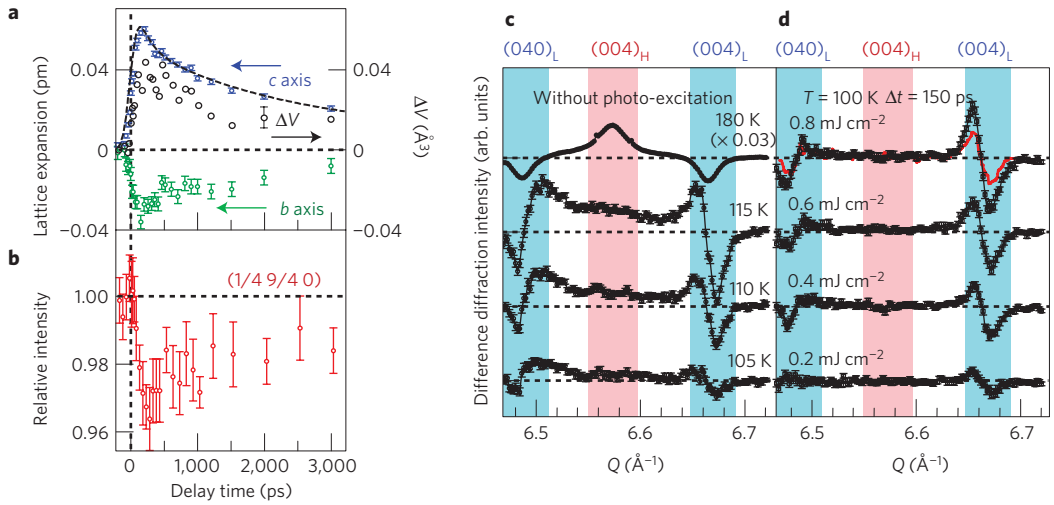

Figure 2 | Photoinduced structural changes at 100 K triggered by irradiation with a 130-fs laser pulse. a, The photoinduced changes in the lattice parameters of the *b* (blue circles) and *c* axes (green circles) and estimated unit cell volume (ΔV) (black circles) as a function of delay time. **b**, The relative intensity of the (1/4 9/4 0) superlattice peak as a function of delay time. Error bars for the lattice constant of the *b* axis are larger than those for the *c* axis because of strong diffraction from the STO substrate. Those for the superlattice become very large because of the weak diffraction intensity. The dashed line in **a** is an exponential decay curve with a lifetime of 3 ns. **c**, Summary of the temperature effects on the DDPs, where the diffraction pattern at 100 K is subtracted from those obtained at various temperatures in a heating run without laser irradiation. **d**, Photoinduced effect on DDPs. The diffraction pattern at 100 K observed immediately before the laser pulse ($\Delta t = -5$ ps) is subtracted from those at $\Delta t = 150$ ps after laser irradiation at various fluences. The temperature and energy density are labelled for each curve in **c** and **d**, respectively. Bars indicate the statistical error. The red curve at the top of **d** shows the DDP observed at $\Delta t = 0$ ps with an excitation fluence of 0.8 mJ cm^{-2}.

of the CO–OO peaks (indicated by the light blue bands). The estimated structural correlation length in the photoexcited state is similar to that before photoexcitation (35 nm, see Supplementary Information), which shows that the photoinduced state can be classified as a single phase.

In addition, Fig. 2c,d shows that the observed photoinduced structural changes, including ΔV, cannot be explained by the thermally perturbed ground state. To achieve the observed lattice constant changes and ΔV value in the ground CO–OO state, a temperature increase of more than 15 K is necessary, as indicated in Fig. 2c. This should also lead to an increase of the diffraction around $Q = 6.58$ Å^{-1} as a result of the appearance of M phase clusters, reflecting the thermodynamic characteristics of NSMO/STO(011). The lack of M phase coexistence in the photoinduced state, despite excess energy injection into the system as a result of ultrafast relaxation processes from the initial photoinduced M phase, also demonstrates large differences in thermodynamic behaviour between the photoinduced and ground states.

As a result of the dynamical X-ray study, it is reasonable to suggest that the observed change in structure and cell volume cannot be attributed to perturbation of the original CO–OO phase by thermal excitation due to injected excess photon energy. Rather, these changes indicate the appearance of a new phase with a homogeneous and well ordered structure. The observed discrepancy in thermodynamic behaviour, that is the lack of phase coexistence in the photoinduced state, also strongly supports this idea. In addition, the intensity of the superlattice Bragg peak in Fig. 2b follows a temporal evolution similar to the changes in lattice constants, with a maximum intensity reduction of about 3%. This shows that the Jahn–Teller distortion seems to be slightly modified but remains well-ordered, even in the photoinduced phase. Therefore, it is a reasonable idea to assign the photoinduced state as a hidden phase in the PIPT process with a Jahn–Teller distortion common to the CO–OO phase.

The observed new structure of this photoinduced phase may relate to hitherto unobserved ground states that could appear by tuning the dimensionality of the Mn–O network[12] and/or by the application of homogeneous, but anisotropic, pressure along the *b* axis. This should be a subject of further study.

Figure 3a–d shows the change in the imaginary part of the dielectric constant ($\Delta\varepsilon_2$) at each probe photon energy after 1.55 eV (800 nm) excitation. The response immediately after photoexcitation, that is at a delay time $\Delta t = 0.1$ ps (Fig. 3a), seems to be consistent with the IM transition, in that it shows a partial conversion from an insulating CO–OO state to a metallic phase, as indicated by the solid line. The observed spectral change at $\Delta t = 0.1$ ps is typical of Mott insulators under photoexcitation and thus is not unique to manganites[25].

However, the emergence ($\Delta t = 150$ ps, Fig. 3c) of a $\Delta\varepsilon_2$ peak around 0.5 eV is atypical. The green dots in Fig. 1e indicate the estimated ε_2 spectrum for 150 ps after photoexcitation using $\Delta\varepsilon_2$. The intensity of the $\Delta\varepsilon_2$ band at 0.5 eV grows with a time constant of 250 ps after the initial metallic state disappears, which is consistent with the X-ray data. As shown by TR-XRD data (see Fig. 2c,d), the observed spectral change can never be explained by the formation of metallic nanoclusters due to dynamic, random phase separation.

The excitation intensity dependence of $\Delta\varepsilon_2$ at 0.52 eV observed at $\Delta t = 150$ ps exhibits a clear threshold at 0.3–0.4 mJ cm^{-2} (indicated by the filled blue circles in Fig. 3e). This result also supports the important role of cooperative interactions in the formation of the hidden phase. It also exhibits saturation behaviour at 0.8 mJ cm^{-2} (equivalent to one excitation photon per 60 Mn ions). Such highly efficient photoconversion is evidence of the critical role cooperative effects play in PIPT phenomena. In contrast, the signal at 0.24 eV observed at $\Delta t = 0.1$ ps grows linearly. This is consistent with the photoinjected carrier density being linearly dependent on the excitation intensity.

The obtained spectral results strongly indicate the emergence of a transient insulating state with a CO gap that is slightly lower (about 0.03 eV) than that of the original CO–OO phase. We tentatively assign the observed large photoinduced changes in the optical properties to the appearance of a hidden insulating phase with a Jahn–Teller distortion, as identified by TR-XRD. This

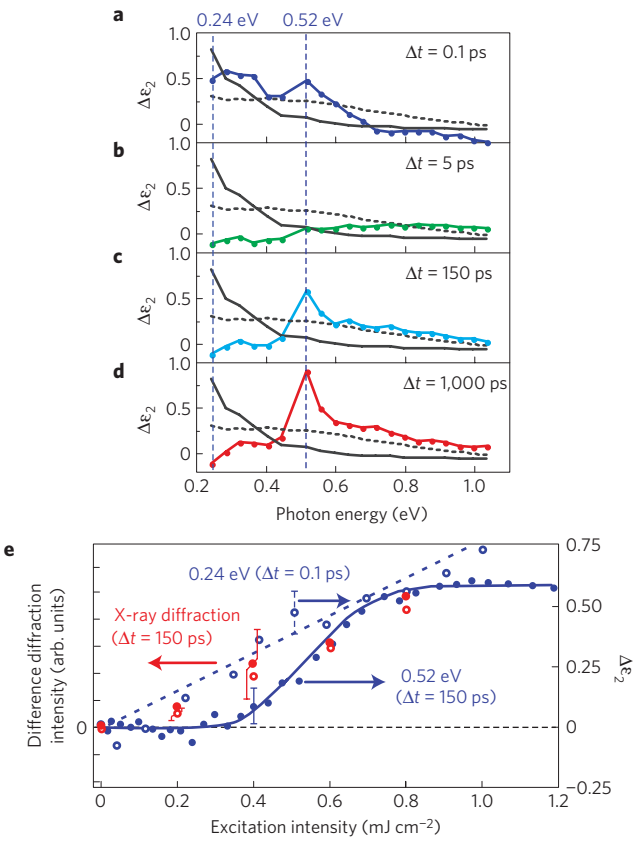

Figure 3 | Photoinduced spectroscopic change at 100 K triggered by irradiation with a 130-fs laser pulse. a–d, Changes in the imaginary part of the dielectric constant observed at delay times (Δt) of 0.1 ps (**a**), 5 ps (**b**), 150 ps (**c**) and 1,000 ps (**d**) after photoexcitation are shown. The solid and dashed lines show simulated spectral changes assuming that 10% of the CO–OO phase at 100 K is converted into the M phase at 180 K and into the CO–OO phase at 140 K, respectively. Dashed blue lines correspond to the photon energies (0.24 and 0.52 eV) used for probing the excitation intensity dependencies of $\Delta\varepsilon_2$ at $\Delta t = 0.1$ ps (for 0.24 eV) and 150 ps (0.52 eV). **e**, Summary of the excitation intensity dependencies of photoinduced signals. The excitation photon density (0.8 mJ cm^{-2}) corresponds to one photon per 60 Mn ions, based on the observed absorbance at the excitation photon energy (1.55 eV). The integrated difference diffraction signal around $Q = 6.65$ Å^{-1} (see Fig. 2d) and the change in superlattice intensity observed 150 ps after photoexcitation are plotted by open and closed red circles, respectively. The total magnitudes of experimental error, including both photon counting statistical error and excitation intensity fluctuation, are shown by dashed and solid red bars. The open and closed blue circles show $\Delta\varepsilon_2$ observed at 0.24 eV at $\Delta t = 0.1$ ps and 0.52 eV at $\Delta t = 150$ ps, respectively. The dashed and solid blue bars also indicate the total experimental errors, due mainly to laser intensity fluctuation. The solid and dashed blue lines are guides for the eye.

result clearly demonstrates that a hidden phase within a complex energy landscape, originating from cooperative interactions, can be accessed using light. This is useful, not only for fundamental studies of non-equilibrium phase transitions, but also for device applications, such as photo-switching materials that have negligible thermal effects and that are damage-free as a result of the large structural changes that occur after photoexcitation.

The microscopic origin of various properties of manganites at low temperature, including their structure, has been discussed in terms of orbital physics. It is reasonable to assume that the microscopic origin of the observed photoeffect on the lattice is the change in orbital polarization. A model calculation relating

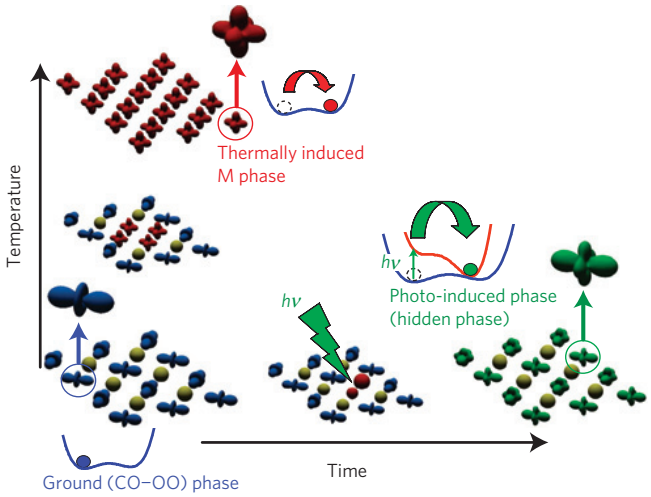

Figure 4 | Schematic illustration contrasting the orbital character of a photoinduced hidden phase with that of a thermally induced M phase converted from the initial CO–OO state (ground state). This is based on the model relation between lattice distortions and orbital polarization in the ground state[19–22]. In the CO–OO state, zigzag-type ordering of $d_{3x^2-r^2}/d_{3y^2-r^2}$ orbitals appears, as indicated by the blue orbitals. In contrast, in the high-temperature M phase, the *d* orbital is nearly isotropic (see red orbitals). A 0.3% increase in the ratio $d_{3z^2-r^2}/(d_{3x^2-r^2}$ or $d_{3y^2-r^2})$ in the CO–OO state (see green orbitals) can explain the observed photoinduced changes in the lattice constants on the basis of the model calculation for the ground state[20,22]. The degree of photoinduced change in the orbital polarization is exaggerated here for clarity. The insets show schematics of free-energy diagrams for the CO–OO, M, and photoinduced 'hidden' phases.

the degree of orbital polarization to the lattice distortion in the ground state[20,22] reveals that a 0.3% increase in the ratio of $d_{3z^2-r^2}/(d_{3x^2-r^2}$ or $d_{3y^2-r^2})$ for 0.8 mJ cm^{-2} excitation can explain the observed lattice changes along the *b* and *c* axes at $\Delta t = 150$ ps (a detailed discussion is given in the Supplementary Information). An estimate of the orbital polarization in the hidden phase using the relation for the ground state is reasonable, because the electron–lattice relaxation occurs within 1 ps and the cooperative lattice distortion subsides in 10 ps (refs 26–29). Hence, the system at $\Delta t = 100$ ps is in a metastable state that can be treated as a hidden phase in 'local' equilibrium. Combining all the observations, Fig. 4 shows a schematic illustration that compares the orbital structure of a photoinduced hidden phase with that of a thermally induced phase.

By combining 100-ps TR-XRD and femtosecond spectroscopy, we have demonstrated that the new photoinduced state, which can be classified as a hidden insulating phase, emerges by relaxation of a precursor metallic state in NSMO/STO(011). The threshold-like behaviour and rather high value in the conversion efficiency, probed by optical methods, supports this idea. Of course, direct probing of the order parameter in charge–orbital–spin coupled systems is the ideal method for definitive identification of a new phase. However, such experimental techniques are difficult to achieve at present, because coupled ultrafast changes in spin, charge and orbital order parameters should be probed simultaneously by using time-resolved resonant X-ray diffraction techniques combined with dynamical probes of the spin structure. In addition, as the red curve in Fig. 2d indicates, the time resolution of the present experimental X-ray system (~100 ps) is too low for studying the initial charge-order melting process[30]. Such attractive subjects are left as future problems awaiting the development of femtosecond TR-XRD techniques.

Methods

Pulsed laser light at 800 nm (1.55 eV) generated from a Ti:sapphire regenerative amplifier system with a pulse width of 130 fs was used to irradiate thin-film NSMO/STO(011) samples at repetition rates of 500 Hz and 945 Hz in optical (1 kHz) and X-ray probe (945 Hz) experiments, respectively. 100-ps TR-XRD experiments, using the single-bunch mode of a storage ring, were carried out at the NW14A beamline in the Photon Factory Advanced Ring, with an X-ray pulse width (full-width at half-maximum (FWHM)) of 100 ps and a repetition rate of 945 Hz. The X-ray energy was set to 15 keV ($\lambda = 0.826$ Å), with an energy bandwidth of 0.01%. The sample was set on a conventional four-circle diffractometer installed in the beamline and the temperature was controlled using a nitrogen-gas-flow cryostat. Diffracted X-rays were detected using a charge-coupled device (CCD) or a scintillation photon detector. Further experimental details and associated references are included in the Supplementary Information.

Received 28 January 2010; accepted 19 November 2010; published online 16 January 2011

References

1. Tokura, Y. Photoinduced phase transition: A tool for generating a hidden state of matter. *J. Phys. Soc. Jpn* **75,** 011001 (2006).
2. Nasu, K. *Photoinduced Phase Transitions* (World Scientific, 2004).
3. Vahaplar, K. *et al.* Ultrafast path for optical magnetization reversal via a strongly nonequilibrium state. *Phys. Rev. Lett.* **103,** 117201 (2009).
4. Lorenc, M. *et al.* Successive dynamical steps of photoinduced switching of a molecular Fe(III) spin-crossover material by time-resolved X-ray diffraction. *Phys. Rev. Lett.* **103,** 028301 (2009).
5. Rini, M. *et al.* Control of the electronic phase of a manganite by mode-selective vibrational excitation. *Nature* **449,** 72–74 (2007).
6. Collet, E. *et al.* Laser-induced ferroelectric structural order in an organic charge-transfer crystal. *Science* **300,** 612–615 (2003).
7. Cavalleri, A., Rini, M & Schoenlein, R. W. Ultra-broadband femtosecond measurements of the photo-induced phase transition in VO_2: From the mid-IR to the hard X-rays. *J. Phys. Soc. Jpn* **75,** 011004 (2006).
8. Kolobov, A. V. *et al.* Understanding the phase-change mechanism of rewritable optical media. *Nature Mater.* **3,** 703–708 (2004).
9. Koshihara, S. & Adachi, S. Photo-induced phase transition in an electron–lattice correlated system—future role of a time-resolved X-ray measurement for materials science. *J. Phys. Soc. Jpn* **75,** 011005 (2006).
10. Huai, P. & Nasu, K. Difference between photoinduced phase and thermally excited phase. *J. Phys. Soc. Jpn* **71,** 1182–1188 (2002).
11. Kajimoto, R. *et al.* Hole-concentration-induced transformation of the magnetic and orbital structures in $Nd_{1-x}Sr_xMnO_3$. *Phys. Rev. B* **60,** 9506–9517 (1999).
12. Okuyama, D. *et al.* Lattice-form-dependent orbital shape and charge disproportionation in charge- and orbital-ordered manganites. *Phys. Rev. B* **80,** 064402 (2009).
13. Tobe, K., Kimura, T. & Tokura, Y. Anisotropic optical spectra of doped manganites with pseudocubic perovskite structure. *Phys. Rev. B* **69,** 014407 (2004).
14. Ogimoto, Y. *et al.* Strain-induced crossover of the metal–insulator transition in perovskite manganites. *Phys. Rev. B* **71,** 060403(R) (2005).
15. Nakamura, M., Ogimoto, Y., Tamaru, H., Izumi, M. & Miyano, K. Phase control through anisotropic strain in $Nd_{0.5}Sr_{0.5}MnO_3$ thin films. *Appl. Phys. Lett.* **86,** 182504 (2005).
16. Miyasaka, K., Nakamura, M., Ogimoto, Y., Tamaru, H. & Miyano, K. Ultrafast photoinduced magnetic moment in a charge–orbital-ordered antiferromagnetic $Nd_{0.5}Sr_{0.5}MnO_3$ thin film. *Phys. Rev. B* **74,** 012401 (2006).
17. Wakabayashi, Y. *et al.* Size of orbital-ordering domain controlled by the itinerancy of the 3*d* electrons in a manganite thin film. *Phys. Rev. B* **79,** 220403(R) (2009).
18. Wakabayashi, Y. *et al.* Orbital ordering structures in $(Nd, Pr)_{0.5}Sr_{0.5}MnO_3$ manganite thin films on perovskite (011) substrates. *J. Phys. Soc. Jpn* **77,** 014712 (2008).
19. Anisimov, V. I., Elfimov, I. S., Korotin, M. A. & Terakura, K. Orbital and charge ordering in $Pr_{1-x}Ca_xMnO_3$ ($x = 0$ and 0.5) from the *ab initio* calculations. *Phys. Rev. B* **55,** 15494–15499 (1997).
20. Maezono, R., Ishihara, S. & Nagaosa, N. Phase diagram of manganese oxides. *Phys. Rev. B* **58,** 11583–11596 (1998).
21. Yunoki, S., Hotta, T. & Dagotto, E. Ferromagnetic, *A*-type, and charge-ordered CE-type states in doped manganites using Jahn–Teller phonons. *Phys. Rev. Lett.* **84,** 3714–3717 (2000).
22. Ebata, K., Mizokawa, T. & Fujimori, A. Orbital ordering in $La_{0.5}Sr_{1.5}MnO_4$ studied by model Hartree–Fock calculation. *Phys. Rev. B* **72,** 233104 (2005).
23. Miyano, K., Tanaka, T., Tomioka, Y. & Tokura, Y. Photoinduced insulator-to-metal transition in a perovskite manganite. *Phys. Rev. Lett.* **78,** 4257–4260 (1997).
24. Dagotto, E. *Springer Series in Solid-State Sciences* 136 (Springer, 2003).
25. Matsubara, M. *et al.* Key for photoinduced insulator–metal transitions in manganites; lattice constant matching between charge/orbital ordered insulator and ferromagnetic metal. *J. Phys. Soc. Jpn* **78,** 023707 (2009).
26. Tamaru, H., Ishida, K, Ogawa, N., Kubo, Y. & Miyano, K. Pump-and-probe study in $LaMnO_3$ thin films. *Phys. Rev. B* **78,** 075119 (2008).
27. Polli, D. *et al.* Coherent orbital waves in the photo-induced insulator–metal dynamics of a magnetoresistive manganite. *Nature Mater.* **6,** 643–647 (2007).
28. Satoh, K. & Ishihara, S. Photo-induced phase transition in charge ordered perovskite manganites. *J. Magn. Magn. Mater.* **310,** 798–800 (2007).
29. Kanamori, Y., Matsueda, H. & Ishihara, S. Dynamical coupling and separation of multiple degrees of freedom in a photoexcited double-exchange system. *Phys. Rev. Lett.* **103,** 267401 (2009).
30. Beaud, P. *et al.* Ultrafast structural phase transition driven by photoinduced melting of charge and orbital order. *Phys. Rev. Lett.* **103,** 155702 (2009).

Acknowledgements

This work was partially supported by Grant-in-Aids for Scientific Research from the MEXT, Japan, and the G-COE programme for chemistry in Tokyo Institute of Technology. This work was carried out with the approval of the Photon Factory Program Advisory Committee (Proposal No. 2004S1-001). The authors thank Y. Okimoto (Tokyo Institute of Technology) for fruitful discussions.

Author contributions

Sample preparation and optical measurements were carried out by Y.O., M.N., R.T. and K.M. H.I. planned the X-ray measurements and carried out the experiment and analysis. S.N., S-i.A., T-h.A. and H.S. planned, conducted and analysed the X-ray measurements; in addition, T.S., A.T., K.I., M.C. and L.G. assisted with the X-ray measurements. N.D. also assisted with the X-ray experiment under the supervision of A.C., as part of the G-COE student exchange program. All authors discussed the results and contributed to the manuscript. S-y.K. and K.M. initiated and oversaw the work.

Additional information

The authors declare no competing financial interests. Supplementary information accompanies this paper on www.nature.com/naturematerials. Reprints and permissions information is available online at http://npg.nature.com/reprintsandpermissions. Correspondence and requests for materials should be addressed to S-y.K.